IEEE Photonics Journal
An IEEE Photonics Society Publication

Open Access

Order-Controllable Cylindrical Vector Vortex Beam Generation by Using Spatial Light Modulator and Cascaded Metasurfaces

Volume 9, Number 5, October 2017

Yanliang He
Huapeng Ye
Junmin Liu
Zhiqiang Xie
Xiaoke Zhang
Yuanjiang Xiang
Shuqing Chen
Ying Li
Dianyuan Fan

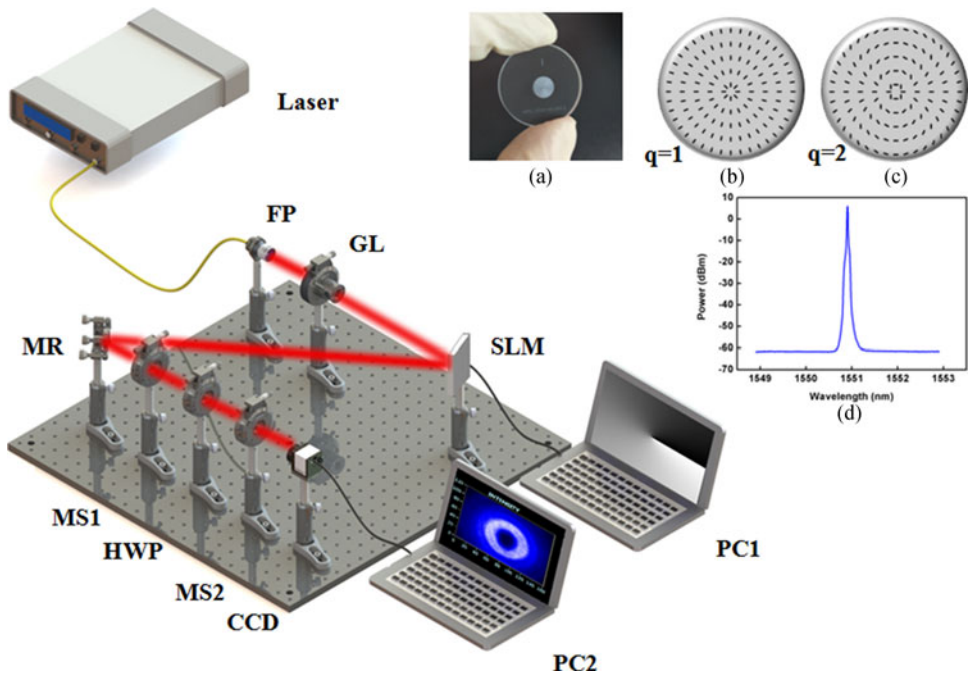

DOI: 10.1109/JPHOT.2017.2741508
1943-0655 © 2017 IEEE

Order-Controllable Cylindrical Vector Vortex Beam Generation by Using Spatial Light Modulator and Cascaded Metasurfaces

Yanliang He,[1] Huapeng Ye,[2] Junmin Liu,[1] Zhiqiang Xie,[1] Xiaoke Zhang,[1] Yuanjiang Xiang,[1] Shuqing Chen,[1] Ying Li,[1] and Dianyuan Fan[1]

[1]International Collaborative Laboratory of 2D Materials for Optoelectronics Science and Technology and Key Laboratory of Optoelectronic Devices and Systems of Ministry of Education and Guangdong Province, Shenzhen University, Shenzhen 518060, China
[2]Department of Electrical and Computer Engineering, National University of Singapore, Singapore 117576

DOI:10.1109/JPHOT.2017.2741508

Manuscript received June 29, 2017; revised July 27, 2017; accepted August 15, 2017. Date of publication August 21, 2017; date of current version September 5, 2017. This work was supported in part by the program of Fundamental Research of Shenzhen Science and Technology Plan under Grants JCYJ20160422152152634, JCYJ2016032814464, and JCYJ20150324141711651, in part by the National Natural Science Foundation of China under Grants 61575127 and 61505122, in part by the project supported by the Guangdong Natural Science Foundation under Grants 2016A030310065 and 2014A030310279, in part by the Natural Science Foundation of SZU under Grants 000059 and 2016031, in part by the Science and Technology Planning Project of Guangdong Province under Grant 2016B050501005, and in part by the Natural Science Foundation Guangdong Education Department under Grants 2015KTSCX124 and 2015KQNCX146. *(Yanliang He and Huapeng Ye contributed equally to this work.)* Corresponding author: Shuqing Chen (e-mail: shuqingchen@szu.edu.cn).

Abstract: Cylindrical vector vortex (CVV) beam, which possesses both helical phase front and spatially inhomogeneous polarization, is a promising structured light for its various applications ranging from optical communication to optical field manipulation and optical microscopy. However, approaches to generate CVV beams with switchable and tunable polarization order and topological charge are still immature, which hinders the wide application of CVV beams. In this paper, we have experimentally demonstrated that order-controllable CVV beams can be produced by using spatial light modulator (SLM) and equivalent *q*-plate system at wavelength of 1550.8 nm. It is shown that the topological charge of the CVV beam can be switched by directly programming the SLM. We have also demonstrated that the polarization order of the CVV beam can be tuned to as high as eight by employing an equivalent *q*-plate system, which consists of two cascaded metasurfaces and a half-wave plate. To further verify the helical phase of the CVV beam, we have proposed a novel measurement method based on first removing the vector property and then interfering the remaining helical phase with plane wave or spherical wave.

Index Terms: Cylindrical vector vortex beam, metasurface, helical phase.

1. Introduction

Cylindrical vector vortex beam, which possesses both helical phase-front and spatially inhomogeneous polarization, has attracted a lot of attentions in recent years [1]–[12]. Compared to scalar

vortex beam, CVV beam not only involves phase singularity and polarization singularity in the beam cross section, but also shows better stability and beam integrity against turbulent atmosphere in free-space transmission [13]. It is well known that both helical phase and inhomogeneous polarization provide a new degree of freedom and thus have been widely applied in optical manipulation [14]–[17], imaging [18]–[21] and communication [22]–[27]. Hence, the CVV beam, which involves aforementioned physical dimensions simultaneously, possesses unprecedented capacities in beam manipulation and inspires various potential applications, especially for the order controllable CVV beams [28]–[30].

Extensive effort has been devoted to exploring the approaches of generating CVV beams. In general, these methods can be classified into three categories, namely method depending on single integrated device [7], generating vortex and vector properties in two separate steps [1], [2], and method by combing two orthogonal circular polarized vortex beams (VB) with different topological charges [3], [4]. In principle, single integrated device can only be used to generate CVV beams with fixed topological charge. As to the second one, the vortex property can be obtained by programming spatial light modulator (SLM) or q-plates. After that, the vector property can be introduced by polarization converters. However, the polarization order introduced by the polarization converter is usually fixed. Although the topological charge of the CVV beam by using the third method is flexible, however, the existing proposals involve complex light path and are always accompanied by low-efficiency. Hence, methods which can conveniently adjusting CVV beam's topological charge and polarization order are highly expected in practical applications. Nevertheless, efficient detection method to independently measure the spiral phase of the CVV beam is still highly demanded.

In this work, we have experimentally demonstrated a novel method to generate CVV beams with controllable order based on the SLM and equivalent q-plate system. It is shown that CVV beams with arbitrary topological charge can be produced by programming the SLM. It is also shown that the polarization order of the CVV beam can be tuned to as large as eight by the equivalent q-plate system consisting of cascaded dielectric metasurfaces and HWP. Moreover, it is found that the radius of the generated CVV beam's hollow-shaped ring increases together with the polarization order and the topological charge of the helical phase. The theoretical prediction based on matrix calculations matches well with the experimental results. Finally, an experimental measurement scheme was proposed to independently measure the helical phase of CVV beams by eliminating the vector property with an equivalent metasurface for optical interference.

2. Theoretical Calculation

Generally, Jones matrix can be used as a tool for theoretical calculation to represent the function of the optical devices. In this article, the Jones matrix of metasurface, which is similar to q-plate in theory, is firstly derived. In the polar coordinate, the direction of the optical axis in the transverse plane can be written as:

$$\phi(r, \theta) = q\theta + \phi_0 \tag{1}$$

Where $\theta = \arctan(y/x)$ is the azimuthal angle, ϕ_0 is the initial direction of the axis, q is a constant indicating the spatial rotation ratio of the optical axis. For simplicity, it is assumed that $\phi_0 = 0$.

Let us consider the metasurface with a homogeneous birefringent phase retardation of π (half-wave) and an inhomogeneous orientation of the fast-optical axis which is parallel to the transverse plane. The Jones matrix of the space-variant metasurface can be simplified as:

$$M(\phi) = \begin{bmatrix} \cos(2\phi) & \sin(2\phi) \\ \sin(2\phi) & -\cos(2\phi) \end{bmatrix} = \begin{bmatrix} \cos(2q\theta) & \sin(2q\theta) \\ \sin(2q\theta) & -\cos(2q\theta) \end{bmatrix} \tag{2}$$

The horizontal linearly polarized light, which can be described with Jones electric-field vector $E_{in} = E_0[1, 0]$, is transformed into the wave as shown in (3) after passing through the metasurface

with q_1,

$$\begin{aligned} E_{\text{out}} &= ME_{\text{in}} \\ &= E_0 \begin{pmatrix} \cos(2\phi) & \sin(2\phi) \\ \sin(2\phi) & -\cos(2\phi) \end{pmatrix} \begin{pmatrix} 1 \\ 0 \end{pmatrix} \\ &= E_0 \begin{pmatrix} \cos(2\phi) \\ \sin(2\phi) \end{pmatrix} \\ &= E_0 \begin{pmatrix} \cos(2q_1\theta) \\ \sin(2q_1\theta) \end{pmatrix} \end{aligned} \tag{3}$$

It is evident that the cylindrical vector beam (CVB) can be obtained with single metasurface. However, the switching operation of CVB's polarization order is unattainable with single metasurface. In order to produce CVV beam with controllable polarization order, we cascade another metasurface with the q-value of q_2, the output wave is then written as:

$$\begin{aligned} E_{\text{out1}} &= ME_{out} \\ &= E_0 \begin{pmatrix} \cos(2q_2\theta) & \sin(2q_2\theta) \\ \sin(2q_2\theta) & -\cos(2q_2\theta) \end{pmatrix} \begin{pmatrix} \cos(2q_1\theta) \\ \sin(2q_1\theta) \end{pmatrix} \\ &= E_0 \begin{pmatrix} \cos(2(q_2 - q_1)\theta) \\ \sin(2(q_2 - q_1)\theta) \end{pmatrix} \end{aligned} \tag{4}$$

By cascading two metasurfaces, the subtraction system can be realized; while the addition system is constituted by inserting a half-wave plate (HWP) between the two metasurfaces with the fast axis parallel to the horizontal axis. After inserting the HWP, the output wave of this system can be represented as:

$$\begin{aligned} E_{\text{out2}} &= MJ_{hw}E_{\text{out}} \\ &= E_0 \begin{pmatrix} \cos(2q_2\theta) & \sin(2q_2\theta) \\ \sin(2q_2\theta) & -\cos(2q_2\theta) \end{pmatrix} \begin{pmatrix} 1 & 0 \\ 0 & -1 \end{pmatrix} \begin{pmatrix} \cos(2q_1\theta) \\ \sin(2q_1\theta) \end{pmatrix} \\ &= E_0 \begin{pmatrix} \cos(2(q_2 + q_1)\theta) \\ \sin(2(q_2 + q_1)\theta) \end{pmatrix} \end{aligned} \tag{5}$$

From (5), we can see that the polarization order of the eventually output CVB is the sum of two metasurfaces. The light wave emerging from the second metasurface has a polarization order of $2(q_2 + q_1)$. By combining both the two metasurfaces and HWP, we can have full control over CVB's polarization order. It should be noted that the different combinations of the two metasurfaces and HWP lead to different equivalent q-plate systems.

When the linearly polarized Gaussian beam is incident into the SLM, the output light beam is $E_0 e^{il\theta}[1, 0]$. The topological charge can be changed if the output beam can be switched by programming the SLM. Hence, we can obtain a large cluster of CVV beams with controllable orders by constructing corresponding equivalent q-plate systems as mentioned above. The obtained CVV beam can be written as

$$E = E_0 e^{il\theta} \begin{pmatrix} \cos(2q\theta) & \sin(2q\theta) \\ \sin(2q\theta) & -\cos(2q\theta) \end{pmatrix} \begin{pmatrix} 1 \\ 0 \end{pmatrix}$$

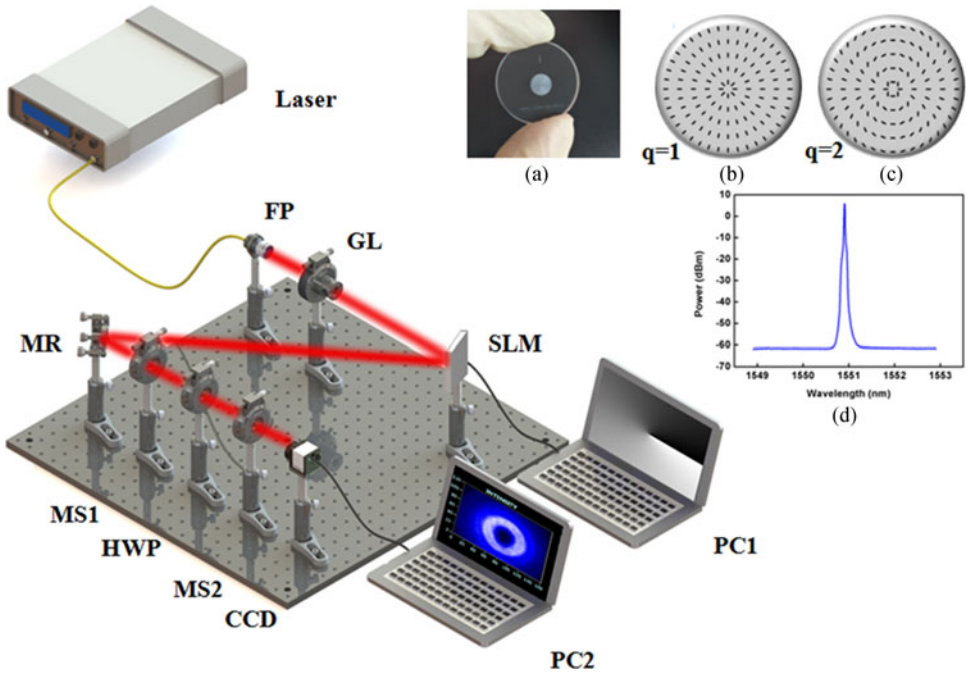

Fig. 1. Experimental setup to generate order-controllable CVV beams. FP: fiber port; GL: Glan laser polarizer; SLM: spatial light modulator; MR: mirror; MS: metasurface; HWP: half-wave plate; CCD: charge coupled device; PC: personal computer. (a) Captured photo of the metasurface we used in the experiment. (b) and (c) Theoretical optical axis distributions of the metasurfaces with $q = 1$ and $q = 2$. (d) Optical spectrum of the monochromatic fundamental Gaussian CW light-wave.

$$= E_0 e^{jl\theta} \begin{pmatrix} \cos(2q\theta) & \sin(2q\theta) \\ \sin(2q\theta) & -\cos(2q\theta) \end{pmatrix} \begin{pmatrix} 1 \\ 0 \end{pmatrix}$$

$$= E_0 e^{jl\theta} \begin{pmatrix} \cos(2q\theta) \\ \sin(2q\theta) \end{pmatrix} \tag{6}$$

Meanwhile, if we want to measure the helical phase of CVV beam independently, we just need to add another q-plate behind the system as above. After that, the output light beam can be written as

$$E = E_0 e^{jl\theta} \begin{pmatrix} \cos(2q\theta) & \sin(2q\theta) \\ \sin(2q\theta) & -\cos(2q\theta) \end{pmatrix} \begin{pmatrix} \cos(2q\theta) \\ \sin(2q\theta) \end{pmatrix} = E_0 e^{jl\theta} \begin{pmatrix} 1 \\ 0 \end{pmatrix} \tag{7}$$

Finally, we can independently measure the helical phase of the CVV beam with the general method of interfering it with plane wave or spherical wave.

3. Results and Discussions

Fig. 1 schematically depicts the experimental setup to generate CVV beams. In the experiment, a fundamental mode Gaussian beam with spectrum as shown in Fig. 1(d) was generated by a continuous wave (CW) laser at wavelength of 1550.8-nm. The laser beam was firstly converted to linearly polarized beam by a Glan laser polarizer (GL). After passing through the SLM which introduces a helical phase to incidence, the linearly polarized beam is converted to VB. With the programmable SLM, we can generate CVV beams with arbitrary topological charge. By combining the VB with the plane wave or the spherical wave with a combiner, the interference patterns of

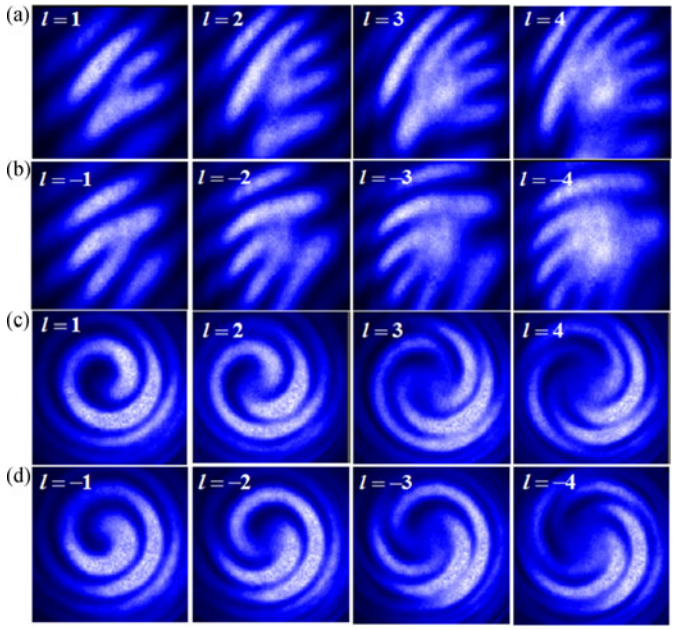

Fig. 2. Measured interference patterns of the generated VBs (topological charges from -4 to $+4$) with plane wave (a)–(b) and spherical wave (c)–(d).

the generated VBs with plane wave and spherical wave were measured respectively, as shown in Fig. 2. The interference patterns between the VB and plane wave are illustrated in Fig. 2(a) and (b). It is evident that the number of dislocated interference fringes is equivalent to the topological charge. When the topological charge is a positive integer, the direction of the fork fringes is oblique upward. Conversely, the direction of the fork fringes is oblique downward when it is negative. The interference patterns with the spherical wave are depicted in Fig. 2(c) and (d), where the number of helical fringes is equivalent to the topological charge. When the topological charge is a positive integer, the rotation direction of helical fringes is anti-clockwise and vice versa.

Optical metasurfaces with micro-sized or nano-sized features have attracted lots of attentions in fields ranging from high-resolution prints, holograph to far-field super-resolution imaging [31]–[33]. Usually, the metasurface is fabricated by etching space-variant grooves on a fused silica sample using a femtosecond laser. The designed grooves are expected to introduce a space-variant birefringence. Desired polarization distribution can be realized by adjusting the local orientation and geometrical parameter of the grooves. As shown in the upper right corner of Fig. 1, the photo and the theoretical optical axis distributions of the metasurfaces are presented. The transmission of metasurface is 90% at the working wavelength of 1550 nm. The effective aperture is 4mm and the conversion efficiency can reach as high as 100%. In the experiment, the metasurface is used to generate CVB. According to [34], q-plate devices placed in the middle of cascaded metasurfaces show arithmetic properties, such as changing the sign of the q-plate, adding two q-plates and subtracting two q-plates. In this paper, we have successfully constructed an equivalent q-plate system by combining the metasurfaces and HWP. The q-value of metasurfaces is 1 and 2, respectively. When the metasurface with q-value of 2 cascades to another one with $q = 2$ or $q = 1$, the q-values of the equivalent q-plate systems are 0 or -1. After inserting a HWP between the two metasurfaces with $q = 1$ and $q = 2$, the q-values of the equivalent q-plate systems is 3. As shown in Fig. 3, the left column shows the vector fields of the five modes, and the second column on the left shows the corresponding intensity distributions without analyzer in front of the CCD. The next three columns show the corresponding intensity distributions with analyzer in front of the CCD, and the polarization angles of the analyzer are indicated at the upper row. The second and third row shows the experimental results of the generated CVBs by using the metasurfaces with $q = 1$ and

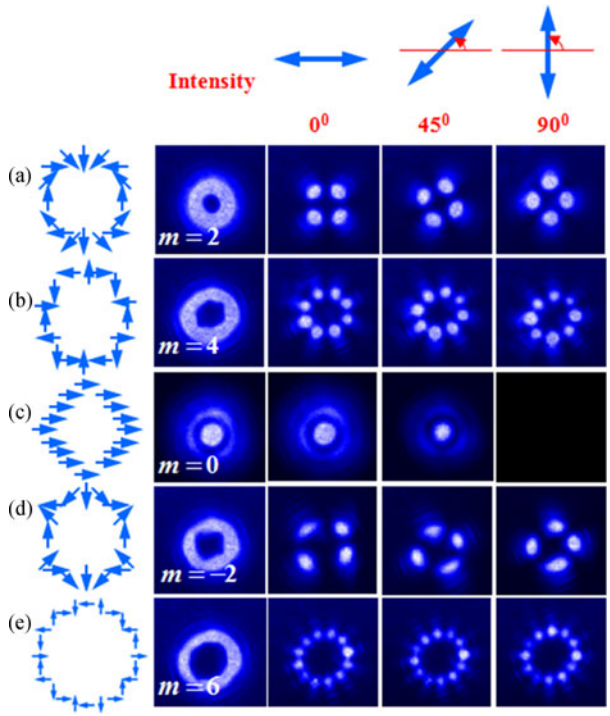

Fig. 3. A set of experimentally generated CVBs with different polarization orders (m) by single metasurface, subtraction and addition operations.

q = 2. The fourth and fifth row shows the intensity profile of output lights, when the q-value of MS1 is 2 and the q-value of MS2 are 2 or 1, respectively. As shown in intensity profile, we can see that the polarization orders (m) of the output lights are 0 and -2. It indicates that the subtraction system is realized. The last row shows the intensity profile of the output light, when the q-value of MS1 is 2 and the q-value of MS2 is 1. After a HWP with fast axis parallel to the horizontal axis is inserted between MS1 and MS2, the subtraction system is transferred into addition system of CVB's polarization order. The polarization order of the output light is 6, as shown in the last row. With the two pairs of metasurfaces with $q = 1$ and $q = 2$, the maximum polarization order can be as high as eight.

In the proposal, the vortex property and the vector property of the CVV beams are introduced by SLM and equivalent q-plate system, respectively. Firstly, the linear polarized Gaussian beam was transformed into linear polarized VB. The topological charge of VB is controllable with programmable SLM. After that the VB is finally transformed into a CVV beam by the equivalent q-plate system which involves different combinations of metasurfaces and HWP. Hence, the SLM and q-plate system constitute a system that can be used for generating order-controllable CVV beams, as depicted in Fig. 4. Fig. 4(a) shows the measured CVV beams without the GL in front of the CCD. The polarization orders (m) are 0, 2, 4, 6 and 8. The topological charges (l) of the helical phases are 0, 1, 2, 3 and 4. It can be found that the diameter of the output light increases together with the polarization order and topological charge. As shown in Fig. 4, the intensity of CVV beam is decreasing with the increase of polarization order and topological charge. On the one hand, the generation of CVV beam with big polarization order involves more devices, thus the efficiency of the whole system would be reduced. On the other hand, the average energy decreased with the increase of diameter of ring-shaped. Fig. 4(b) shows the measured CVV beams with a GL placed in front of the CCD. In general, the analyzer was located in front the CCD to distinguish the CVBs and measure the polarization order of the CVBs. Similar to the differentiating the CVBs, the distinguishment of the CVV beams can be conducted by putting a analyzer in front of the

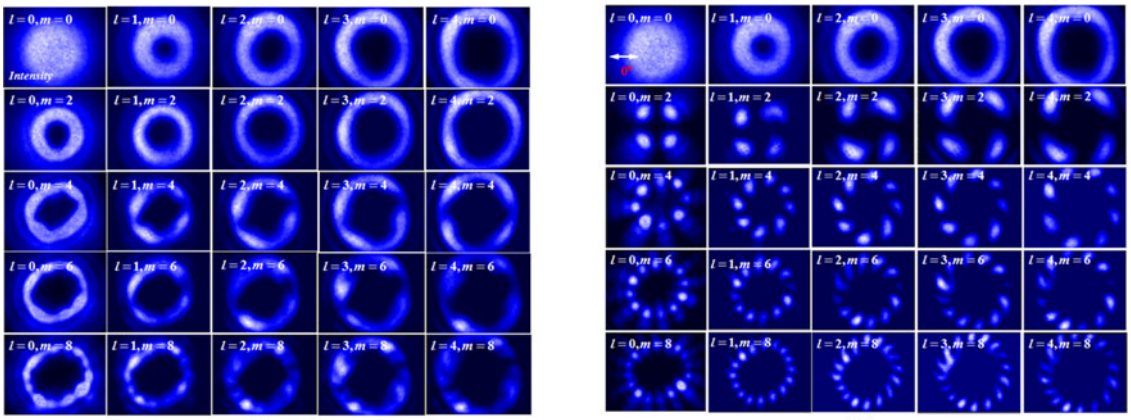

Fig. 4. Measured intensity profiles of CVV beams with different polarization orders (m) and topological charges (l) with (a) or without (b) a GL put in front of the CCD.

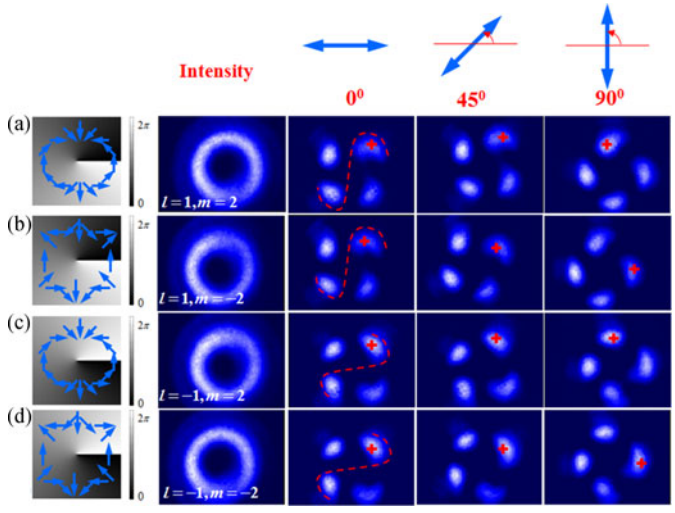

Fig. 5. Measured intensity profiles of CVV beams with opposite sign of polarization orders (m) and opposite sign of topological charges (l) with or without a GL in front of the CCD.

CCD. As shown in the first row of Fig. 4, the ring-shape profile is well maintained as they are just linear polarized VBs. The first column is VBs whose intensity broke up into some light dots that twice the polarization order, which can be also used to measure the polarization orders of the CVV beams. As illustrated in [1], it can be identified that the CVV beam and the sign of topological charge through observing typical "*s*"-shape or anti-"*s*"-shape formed by two light spots on the same diameter. Because both the polarization order and topological charge are larger than one, the middle part of the "*s*"-shape is degraded. However, we can still clearly observe that the light dots drag a little tail except the first column. Therefore, we can confirm that the generated beams are CVV beams based on this phenomenon.

Fig. 5 shows the intensity profile of CVV beams with opposite sign of polarization orders (m) and topological charges (l) when a GL is located in front of the CCD or not. As shown in Fig. 5, when the rotation direction of the light spot which is marked with a red cross is consistent to the rotation direction of the GL' s transmission axis, the sign of polarization order is positive. On the contrary, the sign of polarization order is negative. As shown in the red dotted line, when the pattern formed by two light spots on the same diameter is similar to the "*s*"-shape, the sign of topological

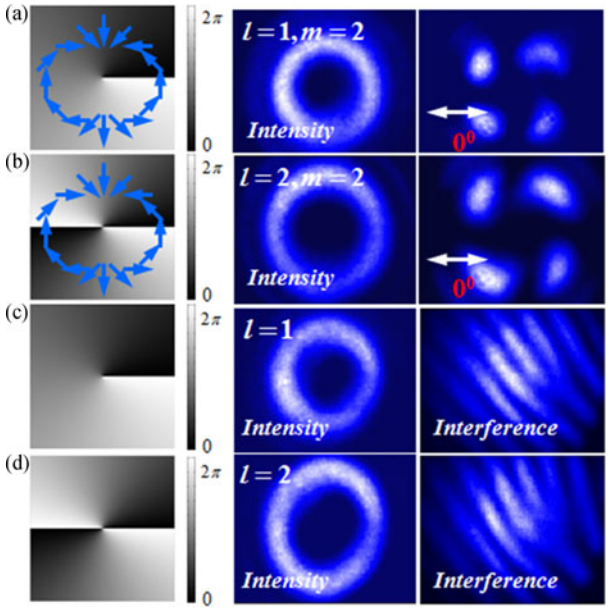

Fig. 6. Experimental results of independently measuring the CVV beams' helical phase with different topological charge (l) +1 (a) and +2 (b), but same polarization order (m). (a) and (b) are the CVV beams under measurement. (c) and (d) are recorded results of the vortex part of the CVV beams, which are prepared to interfere with the coherent plane wave.

charge is positive; when the pattern formed by two light spots on the same diameter is similar to the anti-"*s*"-shape, the sign of topological charge is negative.

As introduced above, we can easily measure the CVV beam's polarization order and the sign of the topological charge with the aforementioned methods. However, we failed to measure the real topological charge of CVV beam, due to the existing of inhomogeneous polarization state under normal interference. Usually, the detection of CVV is realized by decomposing CVV beam into part of left-handed circular polarized and part of right-handed circular polarized, and then their topological charge are detected respectively. Finally, the topological charge is obtained by formula calculation. These methods are relatively complex in experimental setup, and the topological charge of CVV cannot be obtained directly. It is known that the CVV beam is consisting of vortex and vector properties. If we can eliminate the vector properties, the topological charge of the CVV beam can be estimated with common interference method. We have experimental demonstrated that a VB generated from the metasurface can be restored into fundamental Gaussian mode with another metasurface which is placed behind the first metasurface. After the polarization order of the CVV beam is measured by a GL, we can use another metasurface corresponding to the first one to eliminate the vector property of the CVV beam. Then, the topological charge can be measured directly by the interference method. The experimental results to demonstrate our proposal are shown in Fig. 6, where two CVV beams (polarization order m=2) with topological charges (l) of 1 and 2 have been selected. Fig. 6(a) and (b) shows the generated CVV beam. After a GL polarizer was placed before CCD, the ring-shaped of light broke up into four light spots which show that the polarization orders of CVV beams were 2. But it is hard to determine the topological charge of CVV beams. With our proposed measure method, after another equivalent q-plate was used to eliminate the vector property, the rest vortex property of CVV beam interfered with the plane wave. The topological charge of CVV can be determined by interference fringes. As shown in Fig. 6(c) and (d), the measured topological charge is consistent with the real value. Compared to the traditional method, our scheme can obtain topological charge of CVV more directly and much easier to implement. But the polarization order of CVV beam must be measured before we eliminate the vector property of CVV beam with equivalent q-plate.

4. Conclusion

In conclusion, we have experimentally demonstrated that order-controllable CVV beam can be generated by using programmable SLM and equivalent q-plate system. In the experiment, the SLM was used to produce CVV beams with arbitrary topological charge. It is shown that the maximum polarization order of generated CVV beam can be tuned to as high as eight with the equivalent q-plate system which consists of two cascaded metasurfaces and a HWP. It is also shown that the radius of the CVV beam's hollow ring increases together with both polarization order and the topological charge. To independently measure the helical phase of the CVV beam, the vector property of the CVV beam was eliminated by an equivalent metasurface, and meanwhile the beam with reserved vortex property was used to interfere with plane wave or spherical wave for measuring CVV beam's helical phase. The proposed approach for order controllable CVV beam generation may find promising applications in optical communication.

References

[1] X. Yi *et al.*, "Generation of cylindrical vector vortex beams by two cascaded metasurfaces," *Opt. Exp*, vol. 22, no. 14, pp. 17207–17215, Jul. 2014.
[2] Z. Liu *et al.*, "Generation of arbitrary vector vortex beams on hybrid-order Poincaré sphere," *Photon. Res.*, vol. 5, no. 1, pp. 15–21, Feb. 2017.
[3] P. Li *et al.*, "Generation of perfect vectorial vortex beams," *Opt. Lett.*, vol. 41, no. 10, pp. 2205–2208, May 2016.
[4] H. Chen, J. Hao, B. F. Zhang, J. Xu, J. Ding, and H. T. Wang, "Generation of vector beam with space-variant distribution of both polarization and phase," *Opt. Lett.*, vol. 36, no. 16, pp. 3179–3181, Aug. 2011.
[5] D. Zhang, X. Feng, K. Cui, F. Liu, and Y. Huang, "Identifying orbital angular momentum of vectorial vortices with Pancharatnam phase and stokes parameters," *Sci. Rep.*, vol. 5, Jul. 2015, Art. no. 11982.
[6] T. Wakayama *et al.*, "Determination of the polarization states of an arbitrary polarized terahertz beam: Vectorial vortex analysis," *Sci. Rep.*, vol. 5, Mar. 2015, Art. no. 9416.
[7] F. Yue, D. Wen, J. Xin, B. D. Gerardot, J. Li, and X. Chen, "Vector vortex beam generation with a single plasmonic metasurface," *ACS Photon.*, vol. 3, no. 9, pp. 1558–1563, Jul. 2016.
[8] A. D'Errico *et al.*, "Topological features of vector vortex beams perturbed with uniformly polarized light," *Sci. Rep.* vol. 7, Jan. 2017, Art. no. 40195.
[9] C. E. R. Souza, J. A. O. Huguenin, and A. Z. Khoury, "Topological phase structure of vector vortex beams," *J. Opt. Soc. Amer. A*, vol. 31, no. 5, pp. 1007–1012, May 2014.
[10] M. Sakamoto *et al.*, "Polarization grating fabricated by recording a vector hologram between two orthogonally polarized vector vortex beams," *J. Soc. Amer. B*, vol. 34, no. 2, pp. 263–269, Feb. 2017.
[11] F. Cardano, E. Karimi, S. Slussarenko, L. Marrucci, C. D. Lisio, and E. Santamato, "Polarization pattern of vector vortex beams generated by q-plates with different topological charges," *Appl. Opt.*, vol. 51, no. 10, pp. C1–C6, Apr. 2012.
[12] A. Niv, G. Biener, V. Kleiner, and E. Hasman, "Manipulation of the Pancharatnam phase in vectorial vortices," *Opt. Exp*, vol. 14, no. 10, pp. 4208–4220, May 2006.
[13] W. Cheng, J. W. Haus, and Q. Zhan, "Propagation of vector vortex beams through a turbulent atmosphere," *Opt. Exp*, vol. 17, no. 20, pp. 17829–17836, Sep. 2009.
[14] Q. Zhan, "Trapping metallic Rayleigh particles with radial polarization: Reply to comment," *Opt. Exp*, vol. 20, no. 6, pp. 6058–6059, Mar. 2012.
[15] S. Yan and B. Yao, "Radiation forces of a highly focused radially polarized beam on spherical particles," *Phys. Rev. A*, vol. 76, no. 5, Nov. 2007, Art. no. 053836.
[16] G. Rui, X. Wang, and Y. Cui, "Manipulation of metallic nanoparticle with evanescent vortex Bessel beam," *Opt. Exp*, vol. 23, no. 20, pp. 25707–25716, Oct. 2015.
[17] J. Ng, Z. Lin, and C. T. Chan, "Theory of optical trapping by an optical vortex beam," *Phys. Rev. Lett.*, vol. 104, no. 10, Mar. 2010, Art. no. 103601.
[18] Q. Zhan, "Cylindrical vector beams: From mathematical concepts to applications," *Adv. Opt. Photon.*, vol. 1, no. 1, pp. 1–57, Jan. 2009.
[19] A. M. Yao and M. J. Padgett, "Orbital angular momentum: Origins, behavior and applications," *Adv. Opt. Photon.*, vol. 3, no. 2, pp. 161–204, May 2011.
[20] R. Chen, K. Agarwal, C. J. Sheppard, and X. Chen, "Imaging using cylindrical vector beams in a high-numerical-aperture microscopy system," *Opt. Lett.*, vol. 38, no. 16, pp. 3111–3114, Aug. 2013.
[21] D. S. Simon and A. V. Sergienko, "Two-photon spiral imaging with correlated orbital angular momentum states," *Phys. Rev. A*, vol. 85, no. 4, Apr. 2012, Art. no. 043825.
[22] G. Milione *et al.*, "4 $\times$ 20 Gbit/s mode division multiplexing over free space using vector modes and a q-plate mode (de)multiplexer," *Opt. Lett.* vol. 40, no. 9, pp. 1980–1983, May 2015.
[23] Y. Zhao and J. Wang, "High-base vector beam encoding/decoding for visible-light communications," *Opt. Lett.*, vol. 40, no. 21, pp. 4843–4846, Nov. 2015.
[24] G. Milione, T. A. Nguyen, J. Leach, D. A. Nolan, and R. R. Alfano, "Using the nonseparability of vector beams to encode information for optical communication," *Opt. Lett.*, vol. 40, no. 21, pp. 4887–4890, Nov. 2015.

[25] J. Wang *et al.*, "Terabit free-space data transmission employing orbital angular momentum multiplexing," *Nature Photon.*, vol. 6, no. 7, pp. 488–496, Jun. 2012.
[26] G. Gibson *et al.*, "Free-space information transfer using light beams carrying orbital angular momentum," *Opt. Exp,* vol. 12, no. 22, pp. 5448–5456, Oct. 2004.
[27] T. Lei *et al.*, "Massive individual orbital angular momentum channels for multiplexing enabled by Dammann gratings," *Light, Sci. Appl.*, vol. 4, no. 3, Mar. 2015, Art. no. e257.
[28] X. Hao, C. Kuang, T. Wang, and X. Liu, "Phase encoding for sharper focus of the azimuthally polarized beam," *Opt. Lett.*, vol. 35, no. 23, pp. 3928–3930, Dec. 2010.
[29] Z. Zhao, J. Wang, S. Li, and A. E. Willner, "Metamaterials-based broadband generation of orbital angular momentum carrying vector beams," *Opt. Lett.*, vol. 38, no. 6, pp. 932–934, Mar. 2013.
[30] C.-W. Qiu *et al.*, "Engineering light-matter interaction for emerging optical manipulation applications," *Nanophotonics*, vol. 3, no. 3, pp. 181–201, Dec. 2014.
[31] F. Qin *et al.*, "Hybrid bilayer plamonic metasurface efficiently manipulates visible light," *Sci. Adv.*, vol. 2, no. 1, Jan. 2016, Art. no. e1501168.
[32] K. Huang *et al.*, "Ultrahigh-capacity non-periodic photon sieves operating in visible light," *Nature Commun.*, vol. 6, pp. 7059–7065, May 2015.
[33] W. Jiang *et al.*, "Broadband all-dielectric magnifying lens for far-field high-resolution imaging," *Adv. Mater.*, vol. 25, no. 48, pp. 6963–6968, Sep. 2013.
[34] S. Delaney, M. M. Sánchez-López, I. Moreno, and J. A. Davis, "Arithmetic with q-plates," *Appl. Opt.*, vol. 56, no. 3, pp. 596–600, Jan. 2017.